Supplemental Table Legends:

Table S1. Summary of *in vivo* limiting dilution assays. All mice (n=57) injected with CD45+CD19- cells developed MCL-like tumors. Mice implanted with CD45+CD19+ fractions did not develop tumors within the range of injected cells ($5x10^6$ to ~100 cells, n=56 of 57) and in the time course tested, except for one mouse in passage 2 (see *). Tumors from this mouse, however, were much smaller than the xenograft tumors derived from CD45+CD19- fractions. All mice injected with CD45+CD19+ and CD45+CD19- cells were sacrificed at the same time points. Cells were isolated from Pts 1-8. Based on the numbers of mice tested, the frequency of MCL-ICs within CD45+CD19- fractions was at least 1 in 100 cells. The source of tumor cells for second passages were primary passaged tumors generated following CD45+CD19- cell injections.

Table S1.

MCL Source	Cell dose	Primary	Secondary	Tertiary	# of mice with tumors / Total mice injected	Patient sample numbers
Unsorted patient cells	10^7	7			7/7	Pt 3,4,5,8
	10^6	6			6/6	Pt 1,2,6,7
	$5x10^5$	5			5/5	Pt 1,3,5,7
	10^5	5			2/5	Pt 2,4,6
	$5x10^4$	5			2/5	Pt 1,6,8
	10^4	8			2/8	Pt 1,3,4,6,8
	10^3	3			0/3	Pt 1,3,4
CD45+CD19+						
	$5x10^6$	4	2*		1/6	Pt 1,2,7
	10^6	7	6	3	0/16	Pt 4,5,6,8
	$5x10^5$	4	4	3	0/11	Pt 3,5,7
	10^5	3	3		0/6	Pt 1,2,4
	10^4	3	3		0/6	Pt 3,6,8
	10^3	3	3		0/6	Pt 2,3,4
	100	3	2	1	0/6	Pt 1,5,7
CD45+CD19-						
	$5x10^6$	4	2		6/6	Pt 1,2,7
	10^6	7	6	3	16/16	Pt 4,5,6,8
	$5x10^5$	4	4	3	11/11	Pt 3,5,7
	10^5	3	3		6/6	Pt 1,2,4
	10^4	3	3		6/6	Pt 3,6,8
	10^3	3	3		6/6	Pt 2,3,4
	100	3	2	1	6/6	Pt 1,5,7

Supplemental Figure Legends:

Figure S1. Molecular phenotypes of MCL patient PBMC and xenograft tumors.

(A); Absence of Epstein-Barr virus (EBV) in MCL patient samples. PCR analyses were performed with genomic DNA isolated from each patient cells. The Raji B cell line was used as a positive control and the Jeko mantle cell lymphoma cell line was used as a negative control.

(B); Absence of Epstein-Barr virus (EBV) in primary xenograft tumors generated with CD45+CD19- MCL patient cells. PCR analyses were performed with genomic DNA isolated from each cell type. Equal amounts of DNA were used in all samples.

(C); Increased levels of cyclin D1 mRNA were detected in all MCL patient samples. No expression of cyclin D1 was detected in normal blood samples. Cyclin D1 expression was measured via quantitative real time PCR using the following primers: Cyclin D1: F; 5'-GTA TTT GCA TAA CCC TGA GC. R; 5'-GAT GGA ACC TAA TCC TCT CC.

(D); CD45+CD19- cells, but not CD45+CD19+ cells, initiated tumors upon transplantation into NOD/SCID mice. Only mice injected with CD45+CD19- cells developed tumors in the peritoneum of the abdominal wall, thymus, axillary, sacral, mesenteric lymph nodes, or spleens. These data reveal that residual lymphoid tissues in NOD/SCID mice support human lymphoma growth.

Figure S2. Analysis of human MCL cell engraftments in CD45+CD19- and CD45+CD19+ xenograft mice by immunohistochemistry.

(A); Upregulation of cyclin D1 expression was detected in the spleens of CD45+CD19- xenografts (arrows), but not in the spleens of CD45+CD19+ xenografts. All eight patients were examined.

(B); Analysis of CD45 immunostainings of brain, heart, liver, spleen and gut from CD45+CD19+ and CD45+CD19- xenograft mice. The engraftment of CD45+CD19+ cells in all xenograft mice are minimal compared to massive tumors detected in CD45+CD19- xenograft mice.

Figure S3. Additional analysis of human MCL-IC engraftments.

(A); Tumorigenicity of CD45+CD19- MCL-ICs is not dependent on CD34 expression. CD34 staining profiles of CD45+CD19- patient cells (Pt2), which were gated relative to an isotype control (not shown).

(B); Presence or absence of CD34 did not enrich for tumorigenicity of the CD45+CD19- MCL population. The kinetics of xenograft tumor formation in all mice were similar.

(C); MCL patient cells separated by markers other than CD19 did not enrich for tumorigenicity in NOD/SCID mice. CD5 antigen is heterogeneously expressed in MCL patients. APC-CD5 negative FACS gates were determined based on APC-IgG stainings. Pt3 and Pt8 are shown.

(D); FACS profiles of the CD45+CD5+ MCL patient cells before and after CD3 and CD34 depletion revealed that detectable amounts of CD3+ and CD34+ cells were not present after depletion.

(E); CD38, CD5, CD10, and CD69 did not separate tumorigenicity of MCL in NOD/SCID mice. MCL tumors were fractionated using markers other than CD19, and analyzed for tumorigenicity *in vivo*. None of the markers tested were enriched for tumorigenicity of MCL in NOD/SCID mice. MCL-like tumors were formed in all mice and the kinetics of tumor formation

were similar between mice transferred with tumor cells expressing the various markers. FACS and analysis of light chain patterns were performed in all xenograft tumors to ensure they repeated heterogeneity of the original patient cells (data not shown).

(F); Xenograft tumors generated from MCL cells fractionated by markers other than CD19 expression were phenotypically similar to each other. Both cyclin D1 and Ki-67 were upregulated in xenograft tumors generated from the cells differentially expressing CD38 or CD5. Arrows in each panel indicated positive cells. All xenograft tumors showed comparable levels of cell surface marker expression in comparison to the original patient cells (data not shown).

(G); Human MCL cell lines do not contain stem-like cells. CD19 fractionation of Jeko and SP53 MCL cell lines did not enrich for tumor formation. All cell lines formed tumors in mice with similar kinetics, regardless of CD19 fractionation. Tumors were formed in the peritoneum of the abdominal wall, thymus, lymph nodes and spleens (xenograft tumors are not shown).

Figure S1.

A

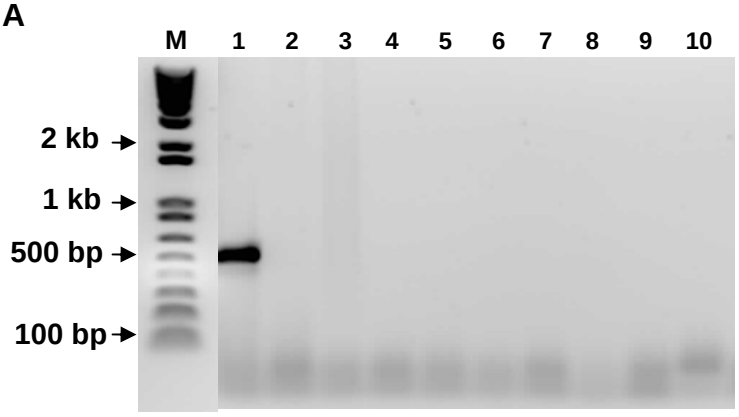

M- Molecular weight marker
1- Raji cells (positive control)
2- Jeko cells (negative control)
3- Pt 1
4- Pt 2
5- Pt 3
6- Pt 4
7- Pt 5
8- Pt 6
9- Pt 7
10- Pt 8

B

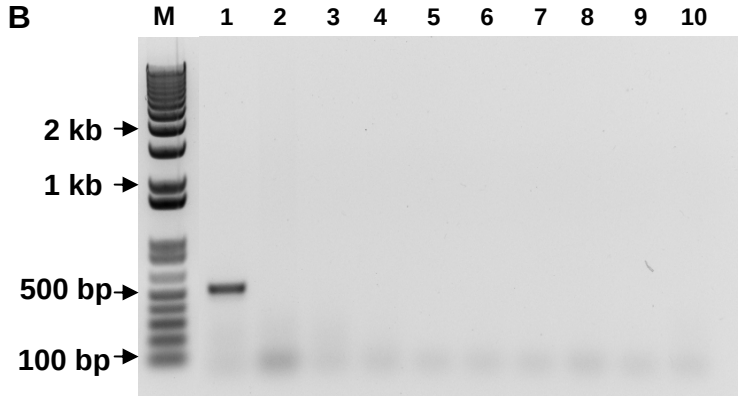

M- Molecular weight marker
1- Raji cells (positive control)
2- Jeko cells (negative control)
3- Xenograft tumors from Pt 1
4- Xenograft tumors from Pt 2
5- Xenograft tumors from Pt 3
6- Xenograft tumors from Pt 4
7- Xenograft tumors from Pt 5
8- Xenograft tumors from Pt 6
9- Xenograft tumors from Pt 7
10- Xenograft tumors from Pt 8

C

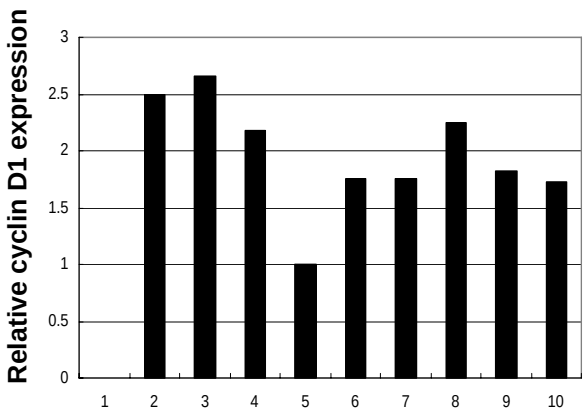

1- Normal PBMC (negative control)
2- Jeko cells (positive control)
3- Pt 1
4- Pt 2
5- Pt 3
6- Pt 4
7- Pt 5
8- Pt 6
9- Pt 7
10- Pt 8

D

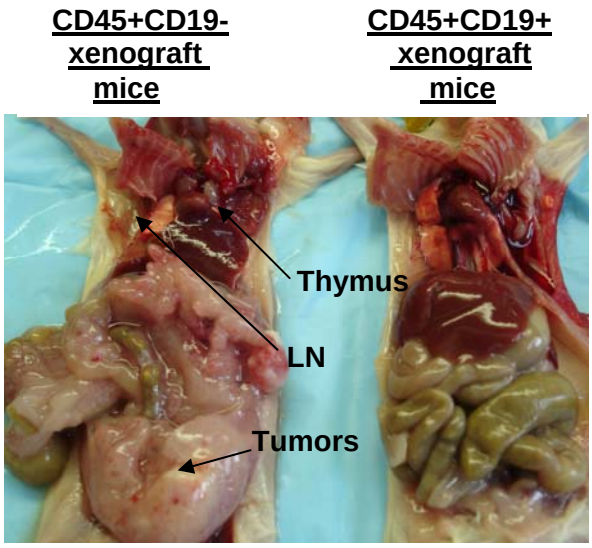
CD45+CD19-
xenograft
mice
CD45+CD19+
xenograft
mice
Thymus
LN
Tumors

Figure S2A.

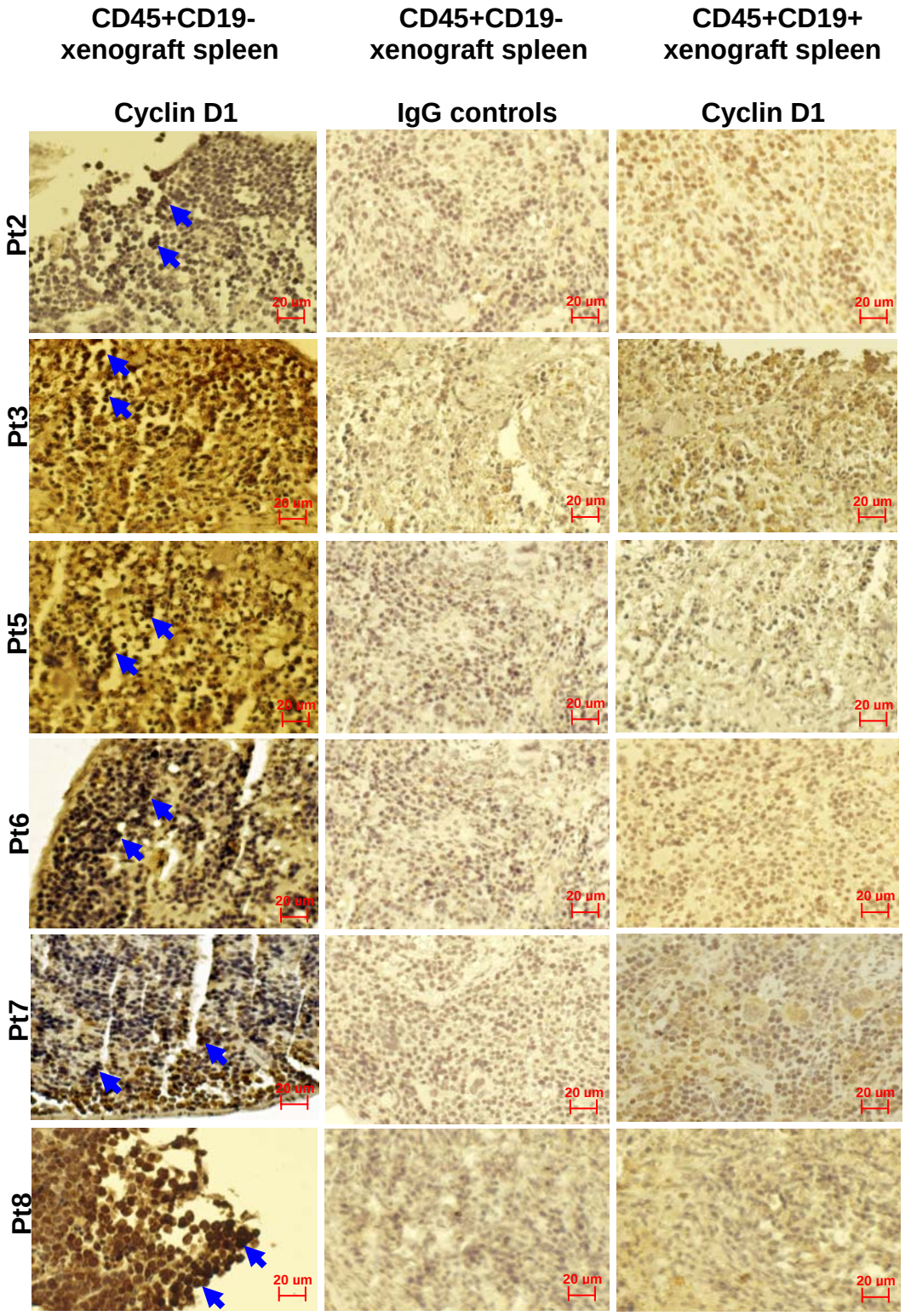
CD45+CD19-
xenograft spleen
Cyclin D1
CD45+CD19-
xenograft spleen
IgG controls
CD45+CD19+
xenograft spleen
Cyclin D1
Pt2
Pt3
Pt5
Pt6
Pt7
Pt8
20 um

Figure S2B.

CD45+CD19+ xenograft mice

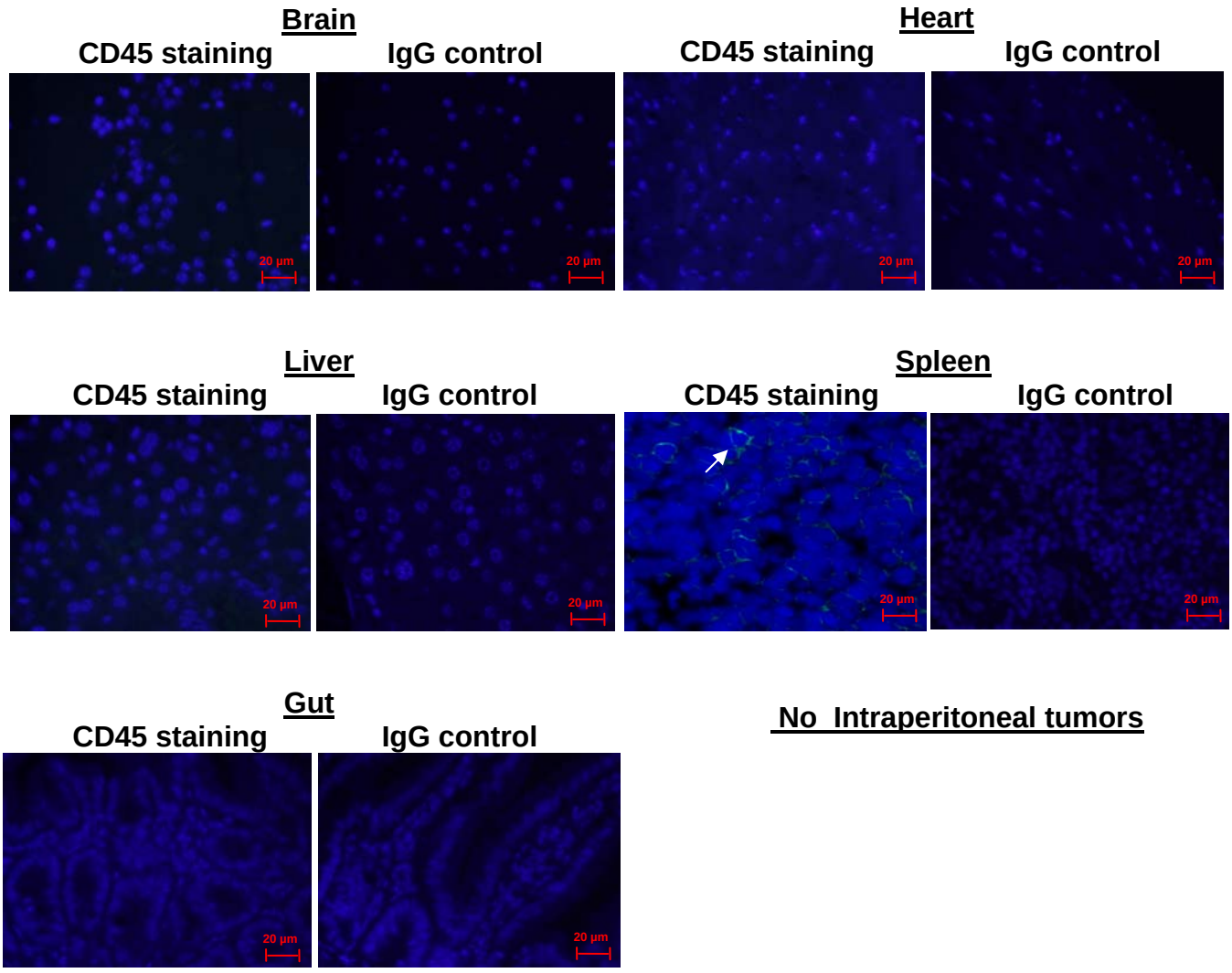

Figure S2B.

CD45+CD19- xenograft mice

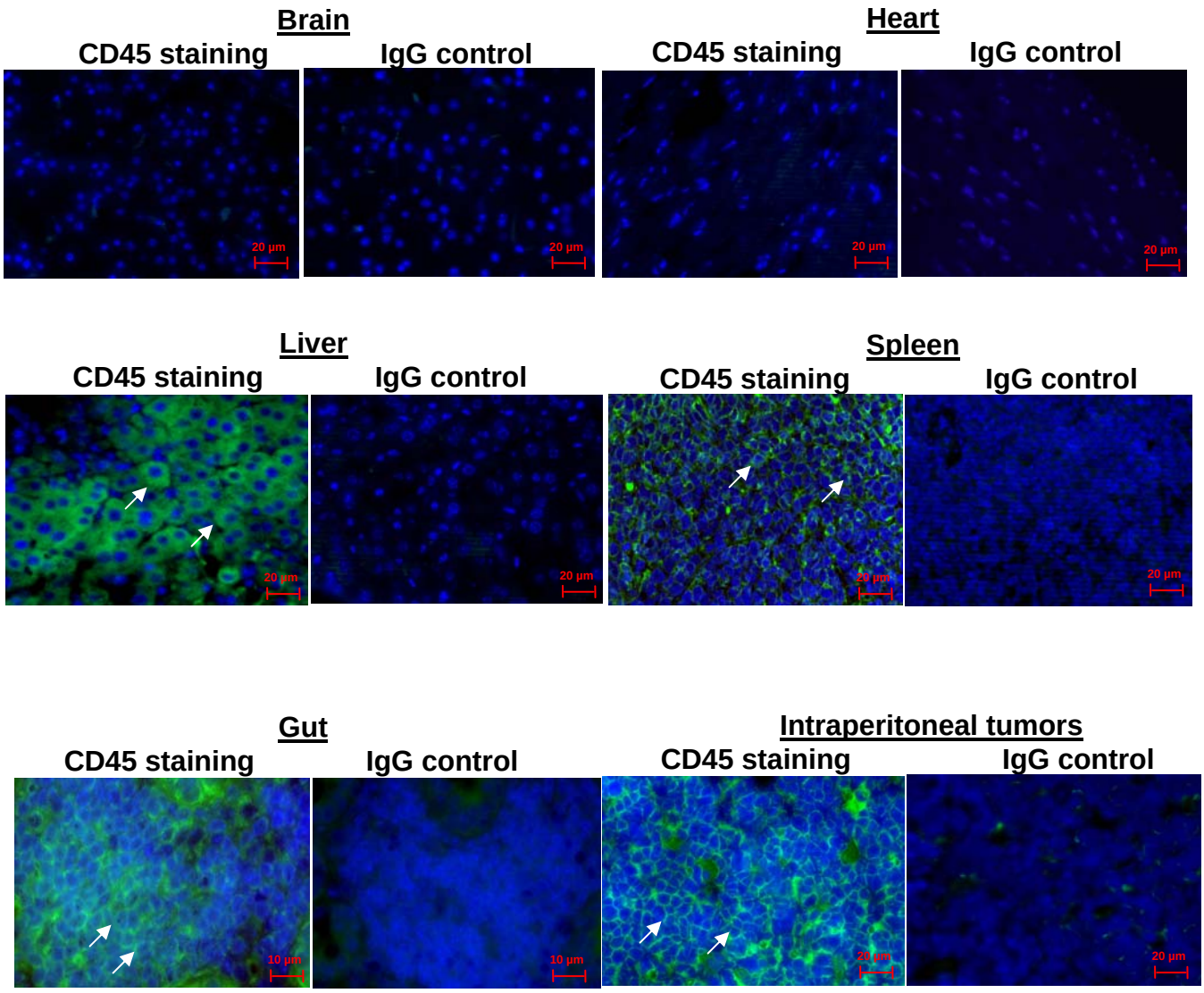

Figure S3A.

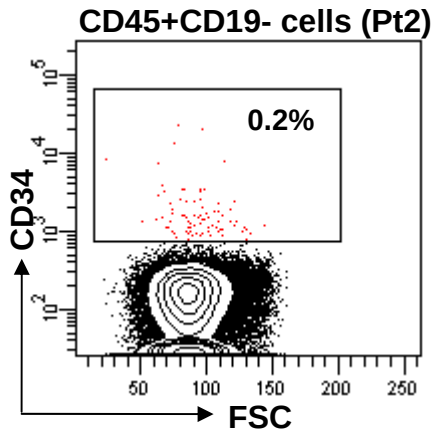

Figure S3B.

Cells injected	Cell dose	# of mice tested	Total # of mice with tumors (%)
CD45+CD19-CD34+	$5x10^6$	1	1/1 (100%)
CD45+CD19-CD34+	10^6	2	2/2 (100%)
CD45+CD19-CD34-	$5x10^6$	1	1/1 (100%)
CD45+CD19-CD34-	10^6	2	2/2 (100%)

Figure S3C.

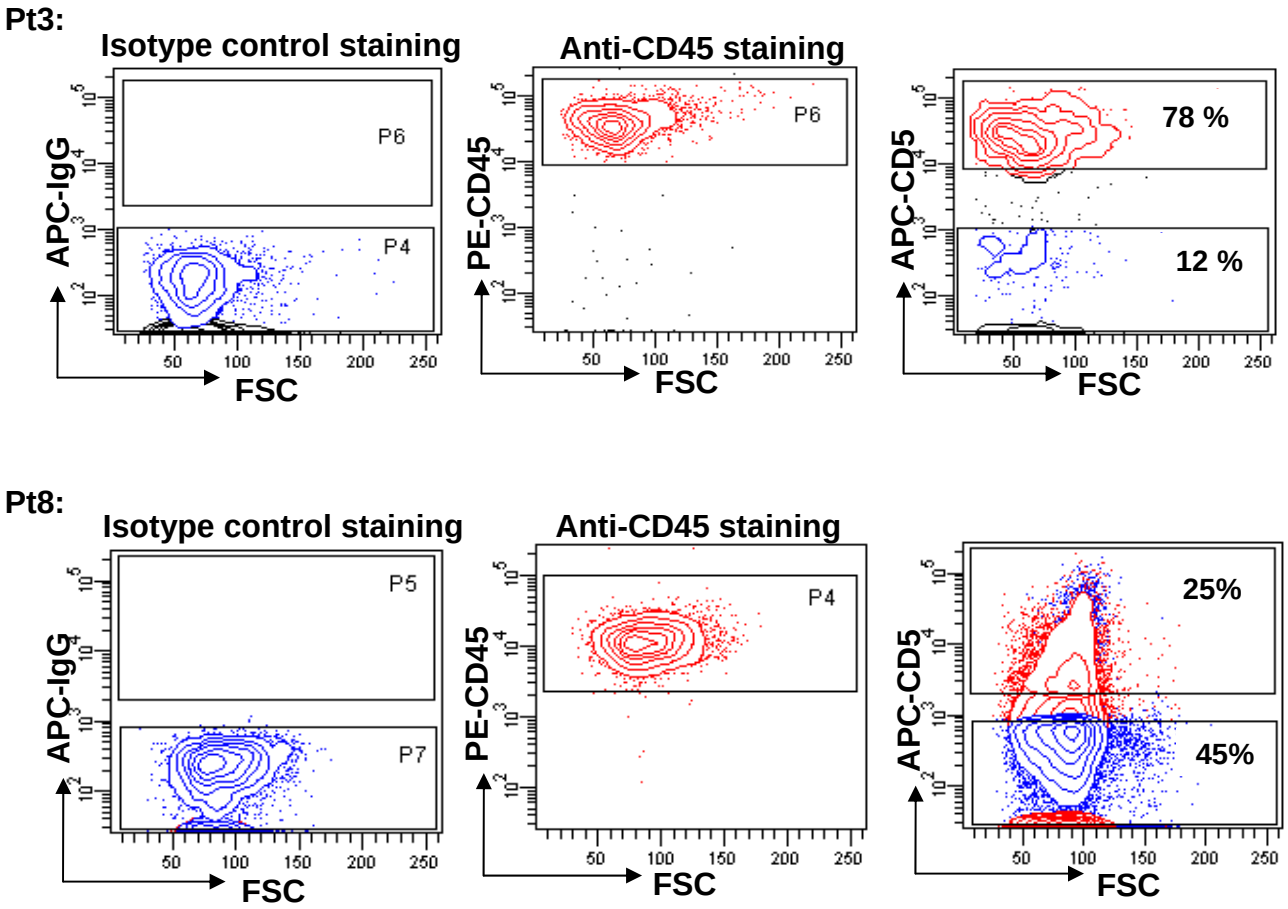
Pt3:
Isotype control staining
Anti-CD45 staining
APC-IgG
PE-CD45
APC-CD5
P6
P4
78 %
12 %
FSC
Pt8:
Isotype control staining
Anti-CD45 staining
P5
P7
P4
25%
45%
50
100
150
200
250

Figure S3D.

Pt 3:

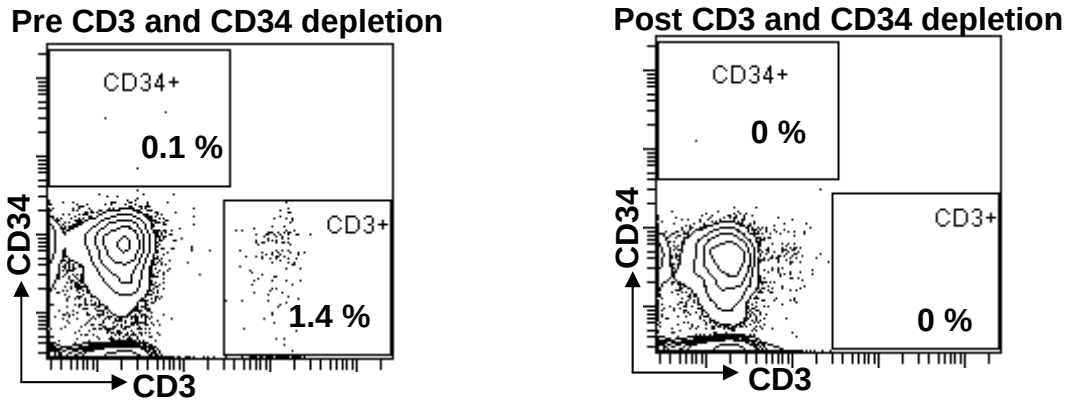

Pt 8:

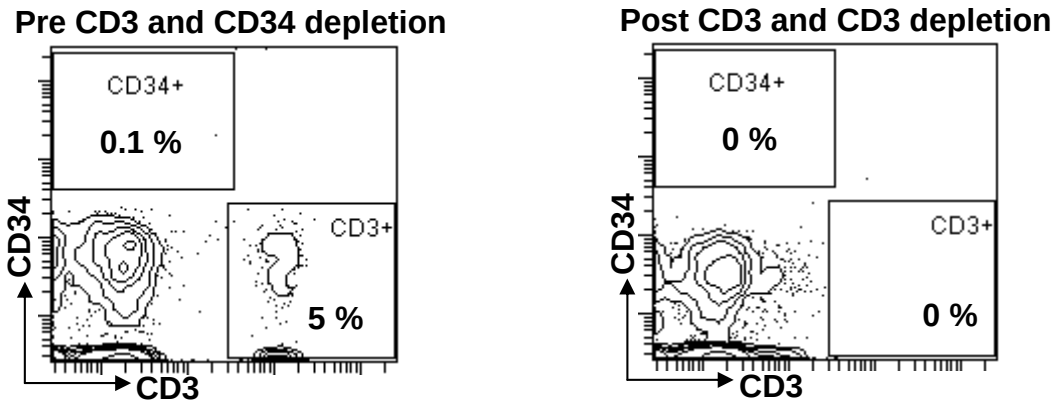

Figure S3E.

Cells injected	Cell dose	# of mice tested	Total # of mice succumbing to tumors
CD45+CD38+	$5x10^5$, $5x\ 10^4$	4	4/4 (100%)
CD45+CD38-	$5x10^5$, $5x10^4$	4	4/4(100%)
CD45+CD5+	$5x10^5$, 10^4	4	4/4 (100%)
CD45+CD5-	$5x10^5$, 10^4	4	4/4 (100%)
CD45+CD10+	$5x10^5$, $5x10^4$	3	3/3 (100%)
CD45+CD10-	$5x10^5$, $5x10^4$	3	3/3 (100%)
CD45+CD69+	$5x10^5$, $5x10^4$	3	3/3 (100%)
CD45+CD69-	$5x10^5$, $5x10^4$	3	3/3 (100%)

Figure S3F.

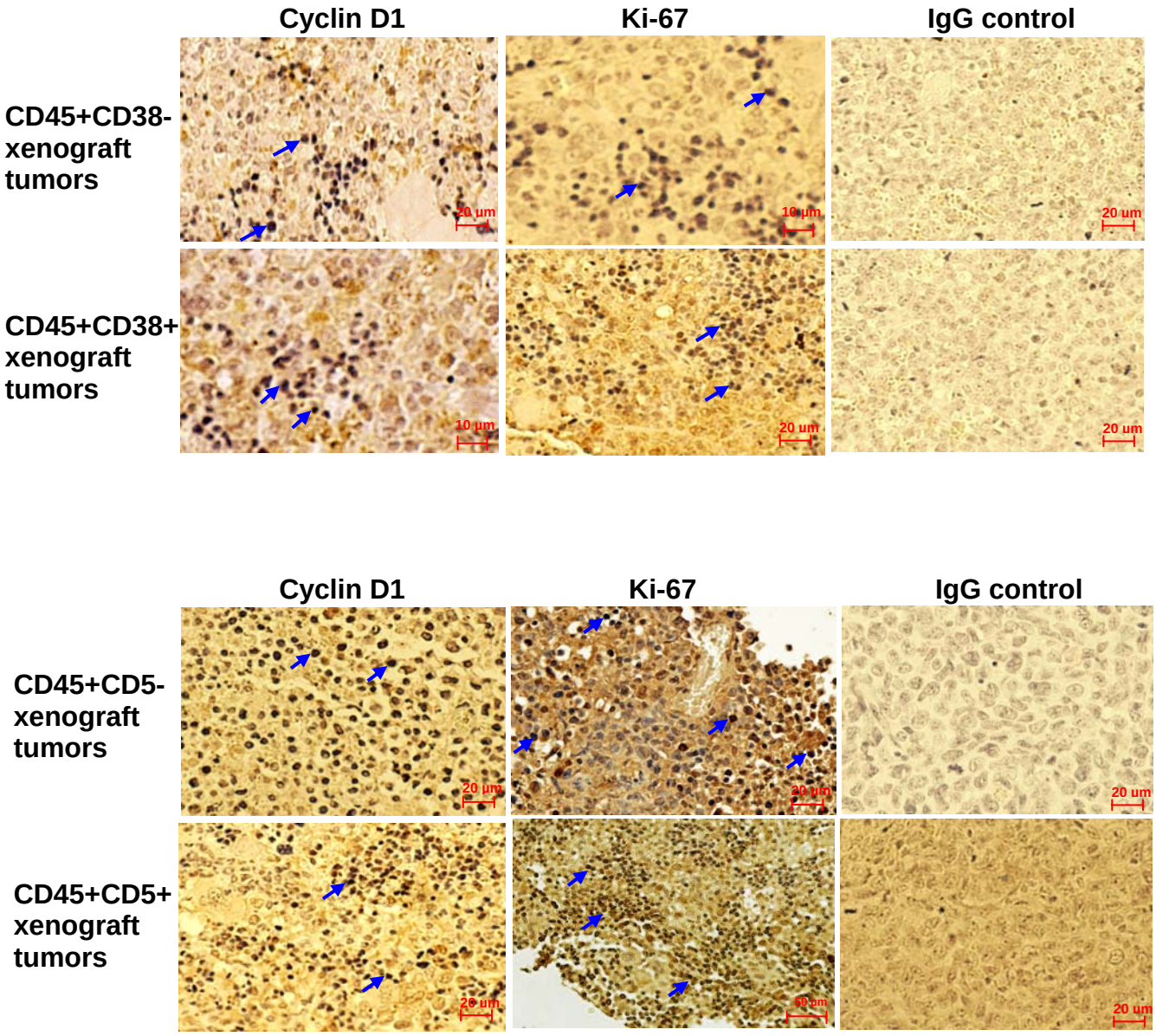
Cyclin D1
Ki-67
IgG control
CD45+CD38- xenograft tumors
CD45+CD38+ xenograft tumors
Cyclin D1
Ki-67
IgG control
CD45+CD5- xenograft tumors
CD45+CD5+ xenograft tumors

Figure S3G.

	Cell dose	**# of mice tested**	**Total # of mice succumbing to tumors**
Jeko CD45+CD19+	$5x10^5$, 10^6	3	3/3 (100%)
Jeko CD45+CD19-	$5x10^5$, 10^6	3	3/3 (100%)
SP53 CD45+CD19+	$5x10^5$, 10^6	3	3/3 (100%)
SP53 CD45+CD19-	$5x10^5$, 10^6	3	3/3 (100%)